

# Bayesian Distance Clustering

Leo L Duan<sup>\*</sup> and David B Dunson<sup>†</sup>

## Abstract

Model-based clustering is widely-used in a variety of application areas. However, fundamental concerns remain about robustness. In particular, results can be sensitive to the choice of kernel representing the within-cluster data density. Leveraging on properties of pairwise differences between data points, we propose a class of Bayesian distance clustering methods, which rely on modeling the likelihood of the pairwise distances in place of the original data. Although some information in the data is discarded, we gain substantial robustness to modeling assumptions. The proposed approach represents an appealing middle ground between distance- and model-based clustering, drawing advantages from each of these canonical approaches. We illustrate dramatic gains in the ability to infer clusters that are not well represented by the usual choices of kernel. A simulation study is included to assess performance relative to competitors, and we apply the approach to clustering of brain genome expression data.

**Keywords:** Distance-based clustering; Mixture model; Model-based clustering; Model misspecification; Pairwise distance matrix; Partial likelihood; Robustness.

## 1 Introduction

Clustering is a primary focus of many statistical analyses, providing a valuable tool for exploratory data analysis and simplification of complex data. In the literature, there are two primary approaches – distance- and model-based clustering. Let  $y_i \in \mathcal{Y}$ , for  $i = 1, \dots, n$ , denote the data and let  $d(y, y')$  denote a distance between data points  $y$  and  $y'$ . Then, distance-based clustering algorithms are typically applied to the  $n \times n$  matrix of pairwise distances  $D_{(n) \times (n)} = \{d_{i,i'}\}$ , with  $d_{i,i'} = d(y_i, y_{i'})$  for all  $i, i'$  pairs. For a recent review, see Jain (2010). In contrast, model-based clustering (Fraley and Raftery, 2002) takes a likelihood-based

---

<sup>\*</sup>Department of Statistics, University of Florida

<sup>†</sup>Department of Statistical Science, Duke University

approach in building a model for the original data  $y_{(n)}$  with  $(n) = \{1, \dots, n\}$  that has the form:

$$y_i \stackrel{iid}{\sim} f, \quad f(y) = \sum_{h=1}^k \pi_h \mathcal{K}(y; \theta_h), \quad (1)$$

where  $\pi = (\pi_1, \dots, \pi_k)'$  is a vector of probability weights in a finite mixture model,  $h$  is a cluster index, and  $\mathcal{K}(y; \theta_h)$  is the density of the data within cluster  $h$ . Typically,  $\mathcal{K}(y; \theta)$  is a density in a parametric family, such as the Gaussian, with  $\theta$  denoting the parameters. The finite mixture model (1) can be obtained by marginalizing out the cluster index  $c_i \in \{1, \dots, k\}$  in the following model:

$$y_i \sim \mathcal{K}(\theta_{c_i}), \quad \text{pr}(c_i = h) = \pi_h. \quad (2)$$

Using this data-augmented form, one can obtain maximum likelihood estimates of the model parameters  $\pi$  and  $\theta = \{\theta_h\}$  via an expectation-maximization algorithm (Fraley and Raftery, 2002). Alternatively, Bayesian methods are widely used to include prior information on the parameters, and characterize uncertainty in the parameters (Marin et al., 2005).

Distance-based algorithms tend to have the advantage of being relatively simple conceptually and computationally, while a key concern is the lack of characterization of uncertainty in clustering estimates and associated inferences. While model-based methods can address these concerns by exploiting a likelihood-based framework, a key disadvantage is large sensitivity to the choice of kernel  $\mathcal{K}(\cdot; \theta)$ . Often, kernels are chosen for simplicity and computational convenience and they place rigid assumptions on the shape of the clusters, which are not justified by the applied setting being considered.

We are not the first to recognize this problem, and there is a literature attempting to improve issues with kernel robustness in model-based clustering. One direction is to choose a flexible class of kernels, which can characterize a wide variety of densities. For example, one can replace the Gaussian kernel with a more flexible class that accommodates asymmetry, skewness and/or heavier tails (Karlis and Santourian, 2009; Juárez and Steel, 2010). A related direction is to nonparametrically estimate the kernels specific to each cluster, while placing minimal constraints for identifiability, such as unimodality and sufficiently light tails. This direction is related to the mode-based clustering algorithms of Li et al. (2007); see also Rodríguez and Walker (2014) for a Bayesian approach using unimodal kernels. Unfortunately, using highly flexible classes of kernels leads to daunting computational issues and a large number of parameters, which rule out the regular use of such approaches in practice.

An alternative strategy is replace the likelihood with a robust alternative. Coretto and Hennig (2016) propose a pseudo-likelihood based approach for robust multivariate clustering, which captures outliers with an extra improper uniform component. Miller and Dunson (2018) propose a coarsened Bayes approach for

robustifying Bayesian inference and apply it to clustering problems. Instead of assuming that the observed data are exactly generated from (1) in defining a Bayesian approach, they condition on the event that the empirical probability mass function of the observed data is within some small neighborhood of that for the assumed model. Both of these methods aim to allow small deviations from a specific type of kernel, which does not completely eliminate sensitivity to the kernel and raises some issues in terms of calibration of how close is close.

We propose a very different approach based on a Bayesian model for the pairwise distances, avoiding a complete specification of the likelihood function for the data  $y_{(n)}$ . There is a rich literature proposing Bayesian approaches that replace an exact likelihood function with some alternative. Chernozhukov and Hong (2003) consider a broad class of such quasi-posterior distributions. Jeffreys (1961) proposed a substitution likelihood for quantiles for use in Bayesian inference; refer also to Dunson and Taylor (2005). Hoff (2007) proposed a Bayesian approach to inference in copula models, which avoids specifying models for the marginal distributions via an extended rank likelihood. Johnson (2005) proposed Bayesian tests based on modeling frequentist test statistics instead of the data directly. These are just some of many such examples.

Our proposed Bayesian Distance Clustering approach gains some of the advantages of model-based clustering, such as uncertainty quantification and flexibility, while significantly improving robustness and simplifying computation in broad problems.

## 2 Partial likelihood for distances

### 2.1 Motivation and partial likelihood

Suppose that data  $y_{(n)}$  are generated from model (1) or equivalently (2). We focus on the case in which  $y_i = (y_{i,1}, \dots, y_{i,p})' \in \mathcal{Y} \subset \mathbb{R}^p$ . The conditional likelihood of the data  $y_{(n)}$  given clustering indices  $c_{(n)}$  can be expressed as

$$L(y_{(n)}; c_{(n)}) = \prod_{h=1}^k \prod_{i:c_i=h} \mathcal{K}_h(y_i) = \prod_{h=1}^k L_h(y^{[h]}), \quad (3)$$

where we let  $\mathcal{K}_h(y)$  denote the density of data within cluster  $h$ , and  $y^{[h]} = \{y_i : c_i = h\} = \{y_i^{[h]}, i = 1, \dots, n_h\}$  is the data in cluster  $h$ . Since the information of  $c_{(n)}$  is stored by the index with  $[h]$ , we will omit  $c_{(n)}$  in the notation when  $[h]$  appears. Referring to  $y_1^{[h]}$  as the *seed* for cluster  $h$ , we can express the likelihood

$L_h(y^{[h]})$  as

$$\begin{aligned} L_h(y^{[h]}) &= \mathcal{K}_h(y_1^{[h]}) \prod_{i=2}^{n_h} G_h(y_i^{[h]} - y_1^{[h]} \mid y_1^{[h]}) \\ &= \mathcal{K}_h(y_1^{[h]} \mid d_{2,1}^{[h]}, \dots, d_{n_h,1}^{[h]}) G_h(d_{2,1}^{[h]}, \dots, d_{n_h,1}^{[h]}) \end{aligned} \quad (4)$$

where  $G_h$  denotes the density of the difference  $d_{i,1}^{[h]} = y_i^{[h]} - y_1^{[h]}$ . Expression (4) is a product of the densities of the seed and  $(n_h - 1)$  differences. As the cluster size  $n_h$  increases, the relative contribution of the seed density  $\mathcal{K}_h(y_1^{[h]} \mid \cdot)$  will decrease and the likelihood becomes dominated by  $G_h$ . The term  $\mathcal{K}_h(y_1^{[h]} \mid \cdot)$  can intuitively be discarded with little impact on the inferences of  $c_{(n)}$ .

Our interest is to utilize all the pairwise differences  $D^{[h]} = \{d_{i,i'}^{[h]}\}_{(i,i')}$ , besides those formed with the seed. Fortunately, there is a linear relationship to determine the other  $d_{i,i'}^{[h]} = d_{i,1}^{[h]} - d_{i',1}^{[h]}$  for all  $i' > 1$ . This means  $\{d_{2,1}^{[h]}, \dots, d_{n_h,1}^{[h]}\}$ , if affinely independent, is a minimal representation (Wainwright and Jordan, 2008) for  $D^{[h]}$ , which is the over-complete representation. As a result, one can induce a density for  $D^{(h)}$  through a density function for  $\{d_{2,1}^{[h]}, \dots, d_{n_h,1}^{[h]}\}$  without restriction. We consider

$$G_h(d_{2,1}^{[h]}, \dots, d_{n_h,1}^{[h]}) = \prod_{i=1}^{n_h} \prod_{i' \neq i} g_h^{\alpha_h}(d_{i,i'}^{[h]}), \quad (5)$$

where  $g_h : \mathbb{R}^p \rightarrow \mathbb{R}_+$  and each  $d_{i,i'}^{[h]}$  is assigned a marginal density. To calibrate the effect of the over-completeness on the right hand side, we use a power parameter  $\alpha_h = 1/n_h$ , with its value justified in the next section.

Slightly abusing notation, we use  $G_h(D^{[h]})$  for (5) from now on. From the assumption that data within a cluster are iid, we can immediately obtain several key properties of  $d_{i,i'}^{[h]} = y_i^{[h]} - y_{i'}^{[h]}$ : (1) Expectation zero, and (2) Marginal symmetry with skewness zero; (3) Single mode at zero as long as  $y_i^{[h]}$  is unimodal (Hodges and Lehmann, 1954).

Hence, the distribution of the differences is substantially simpler than the original data distribution  $\mathcal{K}_h$ . To illustrate, Figure 1 plots the histograms of the data and differences based on a skewed Gaussian. This suggests using  $G_h(D^{[h]})$  for clustering will substantially reduce the model complexity and improve robustness.

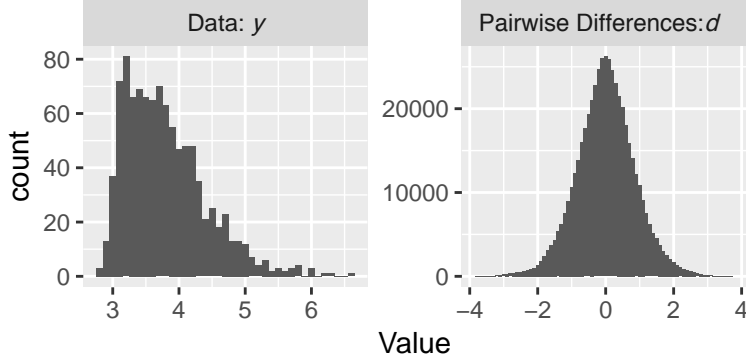


Figure 1: Histograms illustrating properties of pairwise differences within a cluster. Left panel shows the original data  $y_i$  from a right-skewed and shifted Gaussian distribution  $\text{SN}(\mu = 3, \sigma = 1, \alpha = 10)$ ,  $\pi(y_i | \mu, \sigma, \alpha) = 2f\{(y_i - \mu)/\sigma\}F\{\alpha(y - \mu)/\sigma\}$  with  $f$  and  $F$  the density and cumulative distribution functions for standard Gaussian; the right panel shows that its pairwise differences  $d_{i,i'} = y_i - y_{i'}$  for  $i < i'$  are centered at 0 and symmetric.

Lastly, note the differences are closely related to the notion of ‘distance’  $\tilde{d} \in [0, \infty)$ , as a broad concept including metrics, semi-metrics and divergences — the density  $g(\cdot)$  can often be re-parameterized using a distance representation  $\tilde{d}(d_{i,i'})$ , where  $\tilde{d}: \mathbb{R}^p \rightarrow [0, \infty)$ . For example, a multivariate Gaussian density of  $d_{i,i'}^{[h]}$  is equivalent to using Euclidean  $\tilde{d}_{i,i'}^{[h]} = \|d_{i,i'}^{[h]}\|_2$  or Mahalanobis distance  $\tilde{d}_{i,i'}^{[h]} = \sqrt{d_{i,i'}^{[h]'} S d_{i,i'}^{[h]}}$  with  $S$  a positive definite matrix. Furthermore, one could easily generalize  $d_{i,i'}^{[h]}$  from using subtraction to other pairwise transformation, obtaining a broad class of distances. For example, one can obtain Kullback-Leibler distance for those  $y_i$ ’s in probability simplex  $\{y_i \in (0, 1)^p : \sum_{j=1}^p y_{i,j} = 1\}$ , via  $\tilde{d}_{i,i'} = \sum_{j=1}^p y_{i,j}^{[h]} \log(y_{i,j}^{[h]} / y_{i',j}^{[h]})$ .

Therefore, the density (5) can be considered as the likelihood for a large class of distances. Hence we will refer to it as the *distance likelihood*. Conditional on the clustering labels,

$$L(y_{(n)}; c_{(n)}) = \prod_{h=1}^k G_h(D^{[h]}) \quad (6)$$

with  $c_i \sim \sum_{h=1}^k \pi_h \delta_h$  independently, as is (2).

## 2.2 Properties

We describe several interesting properties for the distance likelihood. The first two establish the coherence.

**Lemma 1.** (Exchangeability) *When the product density (5) is used for all  $G_h(D^{[h]})$ ,  $h = 1, \dots, k$ , the distance likelihood (6) is invariant to the permutation of the indices  $i$*

$$L(y_{(n)}; c_{(n)}) = L(y_{(n^*)}; c_{(n^*)})$$

with  $(n^*) = \{1_*, \dots, n_*\}$  denoting a set of permuted indices.

**Remark 1.** Under this exchangeability property, selecting different seeds does not change the distance likelihood.

**Lemma 2.** (Marginalization) Let  $D_{(n_h) \times (n_h)}^{[h]} = \{d_{i,i'}^{[h]} : i \leq n_h, i' \leq n_h\}$  and  $D_{(n_h+1) \times (n_h+1)}^{[h]} = \{d_{i,i'}^{[h]} : i \leq n_h+1, i' \leq n_h+1\}$ . As a regularity condition, we assume that the space  $\mathcal{Y}$  is compact, and assign  $G_h(D_{(1) \times (1)}^{[h]}) = (\int_{\mathcal{Y}} dy_1^{[h]})^{-1}$  so that  $\int_{\mathcal{Y}} G_h(D_{(1) \times (1)}^{[h]}) dy_1^{[h]} = 1$ . For any  $n_h \geq 1$ , if

$$G_h(D_{(n_h) \times (n_h)}^{[h]}) = \int G_h(D_{(n_h+1) \times (n_h+1)}^{[h]}) d d_{(n_h+1),1}^{[h]},$$

then

$$\mathcal{L}(y_{(n+1)}) = \int_{\mathcal{Y}} \mathcal{L}(y_{(n)}) dy_{n+1},$$

where  $\mathcal{L}(y_{(n)}) = \sum_{c_{(n)} \in \{1, \dots, k\}^n} (\prod_{i=1}^n \pi_{c_i}) \prod_{h=1}^k G_h(D_{(n_h) \times (n_h)}^{[h]}; c_{(n)})$  is the likelihood (6) marginalizing out  $c_{(n)}$ .

**Remark 2.** The regularity condition for  $y_1^{[h]}$  is due to that we discard the original density  $\mathcal{K}(y_1^{[h]})$ , which is equivalent to re-assigning  $y_1^{[h]}$  to a uniform measure over  $\mathcal{Y}$ . Although we assume compactness as a regularity condition to simplify the proof of Lemma 2, in practice compactness is not needed for our methodology.

Based on the linear property of the covariance for  $d_{i,i'}^{[h]} = y_i^{[h]} - y_{i'}^{[h]}$ , one can derive that  $\text{cov}(d_{i,i'}^{[h]}) = \text{cov}(y_i^{[h]}) + \text{cov}(y_{i'}^{[h]}) = 2\text{cov}(y_i^{[h]})$  for  $i \neq i'$  and  $\text{cov}(d_{i,i'}^{[h]}, d_{i'',i'''}^{[h]}) = \text{cov}(y_i^{[h]} - y_{i'}^{[h]}, y_{i''}^{[h]} - y_{i'''}^{[h]}) = \text{cov}(y_i^{[h]})$  for pairwise non-equal indices  $i, i', i''$ . Interestingly, without using any complicated form, the product density (5) yields the same correlation structure.

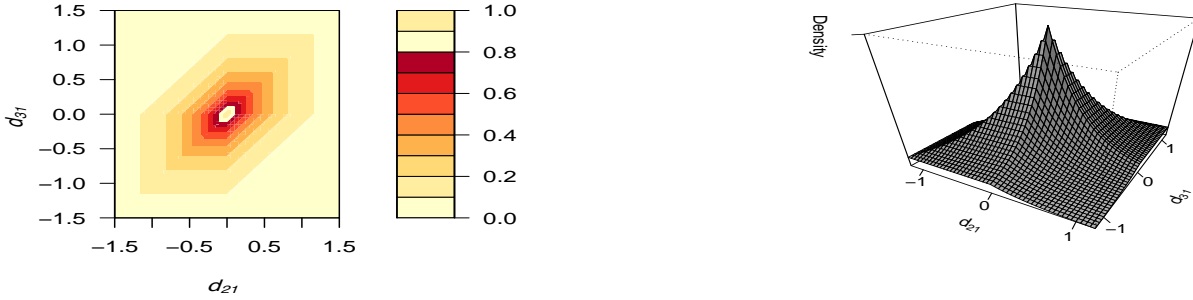
**Lemma 3.** (Correlation) The product density in (5) based on  $d_{i,i'}^{[h]} = y_i^{[h]} - y_{i'}^{[h]}$  has a covariance structure

$$\text{var}(d_{i,i'}^{[h]}) = 2\Sigma, \quad \text{cov}(d_{i,i'}^{[h]}, d_{i'',i'''}^{[h]}) = \Sigma \quad \text{for any } i' \neq i'', i \neq i', i \neq i''$$

where  $\Sigma$  is a  $p$ -by- $p$  positive definite matrix.

**Remark 3.** Typically, within each cluster of a mixture model, in order to model the covariance, one relies on a multivariate Gaussian density for tractability. This lemma shows that we induce a linear dependence structure automatically through our distance likelihood, and hence can focus on a more flexible class of densities for the marginals.

To illustrate, Figure 2 plots the distribution of differences among three data points  $y_1, y_2$  and  $y_3$  in  $\mathbb{R}$ , with a product Laplace density  $G(D) \propto \exp(-|d_{21}|) \exp(-|d_{31}|) \exp(-|d_{32}|)$ . Notice that a correlation is induced between  $d_{21}$  and  $d_{31}$ .



(a) Contour plot of joint density  $d_{21}$  and  $d_{31}$ .

(b) Surface plot of joint density  $d_{21}$  and  $d_{31}$ .

Figure 2: Contour and surface plots showing the product density of the differences formed among  $y_1, y_2$  and  $y_3$ :  $d_{21}$  and  $d_{31}$  are correlated, because the difference  $d_{32} = d_{31} - d_{21}$  is also modeled by the likelihood.

Lastly, we fill the missing gap between the model-based and distance likelihoods though considering an information-theoretic analysis of the two clustering approaches. This also leads to a principled choice of the power  $\alpha_h$  in (5), as mentioned in the last section.

To quantify the information in clustering, we first briefly review the concept of Bregman divergence (Bregman, 1967). Letting  $\phi : \mathcal{S} \rightarrow \mathbb{R}$  be a strictly convex and differentiable function, with  $\mathcal{S}$  the domain of  $\phi$ , the Bregman divergence is defined as

$$B_\phi(x, y) = \phi(x) - \phi(y) - (x - y)' \nabla \phi(y)$$

where  $\nabla \phi(y)$  denotes the gradient of  $\phi$  at  $y$ . A large family of loss functions, such as squared distance and Kullback-Leibler distance are special cases of Bregman divergence with suitable  $\phi$ . For model-based clustering, when the regular exponential family (‘regular’ as the parameter space is a non-empty open set) is used for the component kernel  $\mathcal{K}_h$ , Banerjee et al. (2005) show that there always exists a re-parameterization of the kernel using Bregman divergence. Using our notation,

$$\mathcal{K}_h(y_i; \theta_h) = \exp \{T(y_i)' \theta_h - \psi(\theta_h)\} \kappa(y_i) \Leftrightarrow \exp [-B_\phi \{T(y_i), \mu_h\}] b_\phi \{T(y_i)\},$$

where  $T(y_i)$  is a transformation of  $y_i$ , in the same form as the minimum sufficient statistic for  $\theta_h$  (except this ‘statistic’ is based on only one data point  $y_i$ );  $\mu_h$  is the expectation of  $T(y_i)$  taken with respect to  $\mathcal{K}_h(y; \theta_h)$ ;  $\psi$ ,  $\kappa$  and  $b_\phi$  are functions mapping to  $(0, \infty)$ .

With this re-parametrization, maximizing the model-based likelihood over  $c_{(n)}$  becomes equivalent to minimizing the within-cluster Bregman divergence

$$H_y = \sum_{h=1}^k H_y^{[h]}, \quad H_y^{[h]} = \sum_{i=1}^{n_h} B_\phi \left\{ T(y_i^{[h]}), \mu_h \right\}.$$

We will refer to  $H_y$  as the model-based divergence.

For distance likelihood, since each distance can be viewed or re-parameterized as a pairwise Bregman divergence, we assume each  $g^{\alpha_h}(d_{i,i'}^{[h]})$  in the distance likelihood (5) can be re-parameterized as a scale-class density, with a calibrating power  $\alpha_h > 0$

$$g^{\alpha_h}(d_{i,i'}^{[h]}) = \left(\frac{\kappa}{\lambda_h}\right)^{\alpha_h} \exp \left[ -\frac{\alpha_h}{\lambda_h} B_\phi \left\{ T(y_i^{[h]}), T(y_{i'}^{[h]}) \right\} \right],$$

with  $\lambda_h \in (0, \infty)$  the scale,  $\kappa > 0$  the normalizing constant. A distance-based divergence  $H_d$  can be computed

$$H_d = \sum_{h=1}^k H_d^{[h]}, \quad H_d^{[h]} = \alpha_h \lambda_h^{-1} \sum_{i=1}^{n_h} \sum_{i'=1}^{n_h} B_\phi \left\{ T(y_i^{[h]}), T(y_{i'}^{[h]}) \right\}. \quad (7)$$

We now compare those two divergences at their expectation.

**Lemma 4.** (*Expected Bregman Divergence*) *The distance-based Bregman divergence (7) in cluster  $h$  has*

$$\begin{aligned} \mathbb{E}_{y^{[h]}} H_d^{[h]} &= \alpha_h \lambda_h^{-1} \mathbb{E}_{y_i^{[h]}} \mathbb{E}_{y_{i'}^{[h]}} \sum_{i=1}^{n_h} \sum_{i'=1}^{n_h} B_\phi \left\{ T(y_i^{[h]}), T(y_{i'}^{[h]}) \right\} \\ &= (2n_h \alpha_h \lambda_h^{-1}) \mathbb{E}_{y^{[h]}} \left[ \sum_{i=1}^{n_h} \frac{B_\phi \left\{ T(y_i^{[h]}), \mu_h \right\} + B_\phi \left\{ \mu_h, T(y_i^{[h]}) \right\}}{2} \right], \end{aligned}$$

where the expectation over  $y^{[h]}$  is taken with respect to  $\mathcal{K}_h$ .

**Remark 4.** *The term inside the expectation on the right hand side is the symmetrized Bregman divergence between  $T(y_i^{[h]})$  and  $\mu_h$ , which is close to  $B_\phi \left\{ T(y_i^{[h]}), \mu_h \right\}$  in general (Banerjee et al., 2005). Therefore,  $\mathbb{E}_{y^{[h]}} H_d^{[h]} \approx (2n_h \alpha_h \lambda_h^{-1}) \mathbb{E}_{y^{[h]}} H_y^{[h]}$ ; equality holds exactly if  $B_\phi(\cdot, \cdot)$  is indeed symmetric.*

Notice that the multiplier  $(2n_h \alpha_h \lambda_h^{-1})$  contains a substantial order difference  $\mathcal{O}(n_h)$ , between distance-based and model-based divergences. The parameter  $\lambda_h$ , as the scale for  $B_\phi \left\{ T(y_i^{[h]}), T(y_{i'}^{[h]}) \right\}$ , does not increase with  $n_h$ . Therefore, this difference needs to be manually calibrated – a sensible choice is setting  $\alpha_h = 1/n_h$ . Then, to address the minor constant difference (such as the coefficient 2 and the discrepancy with asymmetric  $B_\phi\{\cdot, \cdot\}$ ), we learn  $\lambda_h$  adaptively from the data by sampling its posterior distribution, using the distance likelihood.



**Remark 5.** The order difference  $\mathcal{O}(n_h)$  is attributed to the use of  $n_h(n_h - 1)$  variables in (5) instead of  $(n_h - 1)$  in its minimal representation. Therefore, we expect this order difference to remain  $\mathcal{O}(n_h)$  even when  $H_y^{[h]}$  and  $H_d^{[h]}$  correspond to slightly different Bregman divergences (e.g. the ones based on Euclidean vs Manhattan distances).

To illustrate the Bregman divergence theory, consider a simple example with data  $y_i^{[h]} \sim \text{No}(\mu_h, \sigma_h^2)$  with  $y_i^{[h]} \in \mathbb{R}$ . The model-based divergence is  $H_y^{[h]} = \sum_i (y_i^{[h]} - \mu_h)^2 / \sigma_h^2$ , and the distance-based divergence using Euclidean distance is  $H_d^{[h]} = (2n_h \alpha_h \lambda_h^{-1}) \sum_{i=1}^{n_h} \sum_{i'=1}^{n_h} (d_{i,i'}^{[h]})^2$ . Having  $\alpha_h = 1/n_h$  and  $\lambda_h = 2\sigma_h^2$  yields  $\mathbb{E}_y H_y^{[h]} = \mathbb{E}_y H_d^{[h]} = n - 1$  exactly. The ideal  $\lambda_h = 2\sigma_h^2$  can be learned using the distance likelihood for  $d_{i,i'}^{[h]}$ , because the variance of  $d_{i,i'}^{[h]}$  is twice as much as the one of  $y_i^{[h]}$  (see the paragraph before Lemma 3).

### 2.3 Choice of Distance Density

To implement the Bayesian distance clustering approach, we need a parametric form for  $g_h(\cdot)$  in (5). Obviously, it imposes some additional assumption about the within-cluster data distribution  $\mathcal{K}_h$ . In order to retain flexibility, we choose to accommodate the potential long tails, assuming that  $\mathcal{K}_h$  corresponds to the class of sub-exponential random variables. This choice covers a large variety of distributions, such as Gaussian, Laplace, Poisson, etc; at the same time, we automatically gain robustness from the un-modeled part, in this case, any non-zero odd moments associated with  $\mathcal{K}_h$  are accommodated.

In considering the choice of a specific density, we first quantify the tail behavior of  $d_{i,i'}^{[h]}$  associated with sub-exponential  $y_i^{[h]}$ . Formally, assuming that each sub-coordinate of  $y_i^{[h]} = (y_{i,1}^{[h]}, \dots, y_{i,p}^{[h]})$  has concentration bound parameter  $\nu_h > 0, b_h > 0$ , characterized by the bound on its moment generating function

$$\mathbb{E} \exp\{t(y_{i,j}^{[h]} - \mu_j^{[h]})\} \leq \exp(\nu_h^2 t^2 / 2) \quad \forall |t| \leq 1/b_h, \quad (8)$$

for  $j = 1, \dots, p$ , where  $\mu_j^{[h]} = \mathbb{E} y_{i,j}^{[h]}$ . It immediately follows that the pairwise difference  $d_{i,i'}^{[h]} = y_i^{[h]} - y_{i'}^{[h]}$  between two iid random variables must be sub-exponential as well, with

$$\mathbb{E} \exp(td_{i,i',j}^{[h]}) \leq \exp(\nu_h^2 t^2) \quad \forall |t| \leq 1/b_h,$$

for  $j = 1, \dots, p$ . To describe the concentration, we now characterize the expectation and its tail probability using its supremum norm. Naturally, the bounds on supremum norm hold for each sub-coordinate of  $d_{i,i',j}^{[h]}$ .

**Lemma 5.** (Concentration of the pairwise difference) If (8) holds, then the supremum norm of each pairwise difference  $\|d_{i,i'}^{[h]}\|_\infty = \max_{j=1}^p |d_{i,i',j}^{[h]}|$  has

$$\begin{aligned} \mathbb{E} \|d_{i,i'}^{[h]}\|_\infty &\leq \max\{2\nu_h \sqrt{\log(2p)}, 2b_h \log(2p)\}, \\ \text{pr}(\|d_{i,i'}^{[h]}\|_\infty > t) &\leq 2p \exp\{-t/(2b_h)\} \quad \text{for } t > 2\nu_h^2/b_h. \end{aligned}$$

The second inequality in Lemma 5 shows that, under small or moderate  $p$ , the tail of  $d_{i,i'}^{[h]}$  can be adequately bounded by the tail of a Laplace distribution up to some constant difference (discussions for large  $p$  are provided in Section 6). Therefore, we use a  $p$ -dimensional Laplace distribution for

$$g_h(d_{i,i'}^{[h]}) = (2\sigma_h)^{-p} \exp\left(-\sum_{j=1}^p |d_{i,i',j}^{[h]}|/\sigma_{h,j}\right),$$

which is equivalent to a function using weighted Manhattan distance  $\tilde{d}_{i,i'}^{[h]} = \|(w_1 d_{i,i',1}^{[h]}, \dots, w_p d_{i,i',p}^{[h]})\|_1$  with  $w_j = \sigma_{h,j}^{-1}/\lambda_h$  and  $\lambda_h = (\sum_j \sigma_{h,j}^{-1})^{-1}$  the scale parameter in the Bregman divergence representation. To allow borrowing of information, we assign  $\sigma_{h,j}^{-1} \stackrel{iid}{\sim} \text{Ga}(3, a_j)$  for  $h = 1 \dots k$  and  $j = 1, \dots, p$ , with  $a_j \sim \text{Ga}(0.1, 0.1)$ . The hyper-parameter  $a_j$  can be estimated from the posterior, whereas the first parameter is fixed to 3 so that the prior  $\text{var}(\sigma_h) < \infty$ . We assign prior for the component weights  $(\pi_1, \dots, \pi_k) \sim \text{Dir}(\alpha, \dots, \alpha)$ .

### 3 Posterior Computation

We use Markov chain Monte Carlo to sample from the posterior distribution. This is based on Gibbs sampling algorithm with the following steps:

1. For  $i = 1, \dots, n$ , sample  $c_i$  according to

$$\text{pr}(c_i = h \mid c_{(n)} \setminus \{c_i\}, D_{(n)}) = \frac{\pi_h G_h\{D_{(n_h) \times (n_h)}^{[h]}\} / G_h\{D_{[(n_h) \setminus \{i\}] \times [(n_h) \setminus \{i\}]}^{[h]}\}}{\sum_{h'=1}^k \pi_{h'} G_{h'}\{D_{(n_{h'}) \times (n_{h'})}^{[h']}\} / G_{h'}\{D_{[(n_{h'}) \setminus \{i\}] \times [(n_{h'}) \setminus \{i\}]}^{[h']}\}}, \quad (9)$$

where  $(n_h) \setminus \{i\}$  are the indices of the data in cluster  $h$  excluding  $y_i$ .

2. For  $h = 1, \dots, k$  and  $j = 1, \dots, p$ , sample

$$\sigma_{h,j}^{-1} \sim \text{Ga}\left\{(n_h - 1) + 3, \sum_{i,i'} |d_{i,i',j}^{[h]}|/n_h + a_j\right\},$$

if  $n_h > 1$ ; otherwise update from  $\sigma_h^{-1} \sim \text{Ga}(3, a_j)$ .

3. For  $j = 1, \dots, p$ , sample  $a_j \sim \text{Ga}(3k + 0.1, \sum_{h=1}^k \sigma_{h,j}^{-1} + 0.1)$ .

4. Sample  $(\pi_1, \dots, \pi_h) \sim \text{Dir}(\alpha + n_1, \dots, \alpha + n_h)$ .

We run the algorithm over iterations  $s = 1, \dots, S$ . To reduce the effects of label-switching, we track the probabilities (9) and post-process the labels as described in Stephens (2000), with processed label denoted by  $\tilde{c}_i^{(s)}$ . To estimate the marginal assignment probability, we use  $\text{pr}(c_i = h) = \sum_{s=1}^S 1(\tilde{c}_i^{(s)} = h)/S$ . To produce a point estimate  $\hat{c}_{(n)}$ , we minimize the variation of information as the loss function, with algorithm provided in Wade and Ghahramani (2018).

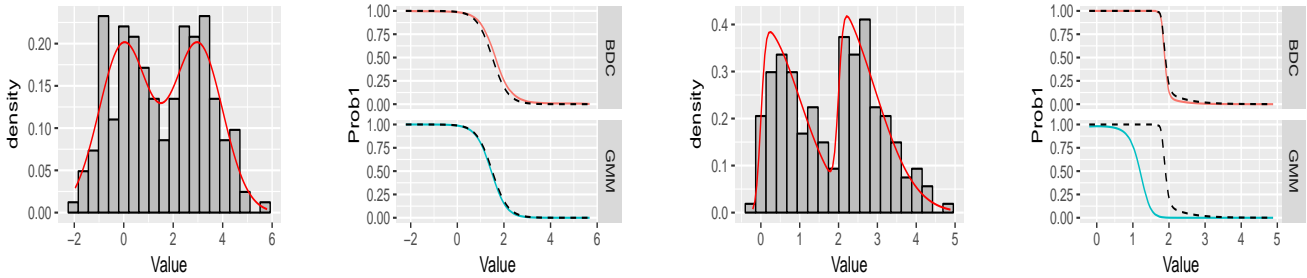
## 4 Simulations

### 4.1 Robustness to Skewed Distribution

We now illustrate that Bayesian distance clustering can automatically accommodate skewness. We generate  $n = 200$  data from a two-component mixture of skewed Gaussians:

$$\begin{aligned} \text{pr}(c_i = 1) &= \text{pr}(c_i = 2) = 0.5, \\ y_{i,j} \mid c_i = h &\sim \text{SN}(\mu_h, 1, \alpha_h) \text{ for } j = 1 \dots p \end{aligned}$$

where  $\text{SN}(\mu, \sigma, \alpha)$  has density  $\pi(y \mid \mu, \sigma, \alpha) = 2f\{(y - \mu)/\sigma\}F\{\alpha(y - \mu)/\sigma\}$  with  $f$  and  $F$  the density and cumulative distribution functions for the standard Gaussian distribution.



(a) Histogram and the true density (red line) of a mixture of two symmetric Gaussians.

(b) Assignment probability  $\text{pr}(c_i = 1)$ , under Bayesian distance clustering and the mixture of Gaussians. Dashed line is the oracle probability based on symmetric Gaussians.

(c) Histogram and the true density (red line) of a mixture of two right skewed Gaussians.

(d) Assignment probability  $\text{pr}(c_i = 1)$ , under Bayesian distance clustering and the mixture of Gaussians. Dashed line is the oracle probability based on skewed Gaussians.

Figure 3: Clustering data from a two component mixture of skewed Gaussians in  $\mathbb{R}$ . Bayesian Distance clustering (BDC) gives posterior clustering probabilities close to the oracle probabilities regardless of whether the distribution is skewed or not (upper plots in panel b and d), while the mixture of Gaussians fails when the skewness is present (lower plot in panel d).

We start with  $p = 1$  and assess the performance of the Bayesian distance clustering model under both non-skewed ( $\alpha_1 = \alpha_2 = 0, \mu_1 = 0, \mu_2 = 3$ ) and skewed distributions ( $\alpha_1 = 8, \alpha_2 = 10, \mu_1 = 0, \mu_2 = 2$ ). The results are compared against the mixture of Gaussians as implemented in the *Mclust* package. Figure 3(a-b) show that for non-skewed Gaussians, the proposed approach produces clustering probabilities

close to their oracle probabilities, obtained using knowledge of the true kernels that generated the data. When the true kernels are skewed Gaussians, Figure 3(c-d) shows that the mixture of Gaussians gives inaccurate estimates of the clustering probability, whereas Bayesian distance clustering remains similar to the oracle.

To evaluate the accuracy of the point estimate  $\hat{c}_i$ , we compute the adjusted Rand index (Rand, 1971) with respect to the true labels. We test under different  $p \in \{1, 5, 10, 30\}$ , and repeat each experiment for 30 times. The results are compared against model-based clustering using symmetric and skewed Gaussians kernels, using independent variance structure. As shown in Table 1, the misspecified symmetric model deteriorates quickly as  $p$  increases; surprisingly, the correctly specified skewed Gaussian also suffers from rapidly worsening performance as  $p$  increases. In contrast, Bayesian distance clustering maintains high clustering accuracy. This drastic difference is likely due to the number of parameters in each cluster: the mixture of skewed Gaussians needs  $3p$  parameters for the location, scale and skewness, while Bayesian distance clustering only needs  $p$  for the scale.

Table 1: Accuracy of clustering skewed Gaussians under different dimensions  $p$ . Adjusted Rand index (ARI) is computed for the point estimates using variation of information. The average and 95% credible interval are shown.

$p$	Bayes Dist. Clustering	Mix. of Gaussians	Mix. of Skewed Gaussians
1	0.80 (0.75, 0.84)	0.65 (0.55, 0.71)	0.81 (0.75, 0.85)
5	0.76 (0.71, 0.81)	0.55 (0.40, 0.61)	0.76 (0.72, 0.80)
10	0.72 (0.68, 0.76)	0.33(0.25, 0.46)	0.62 (0.53, 0.71)
30	0.71 (0.67, 0.76)	0.25 (0.20, 0.30)	0.43 (0.37, 0.50)

## 4.2 Clustering Discrete or Constrained Data

In model-based clustering, if the data are discrete or in a constrained space, one would use a distribution customized to the type of data. For example, one may use the multinomial distribution for categorical data, or the directional distribution (Khatri and Mardia, 1977) for data on a unit sphere. Comparatively, distance clustering is simpler to use, since one can define distances similarly as for unconstrained continuous data.

We will use two examples to illustrate. We first consider multivariate binary outcome  $y_i \in \{0, 1\}^p$  and generate  $n = 400$  data from a two component multivariate Bernoulli mixture:

$$\begin{aligned} \text{pr}(c_i = 1) &= \text{pr}(c_i = 2) = 0.5, \\ y_{i,j} \mid c_i = h &\sim \text{Bern}(q_{h,j}) \text{ for } j = 1 \dots p \end{aligned}$$

for  $i = 1, \dots, n$ , where  $(q_{1,1}, \dots, q_{1,p}) = (0.1, 0.1 + s, \dots, 0.9 - s, 0.9)$  is a vector of probabilities increasing with fixed increment  $s = 0.8/(p - 1)$ , with  $(q_{2,1}, \dots, q_{2,p}) = (0.9, 0.9 - s, \dots, 0.1 + s, 0.1)$  a probability vector in decreasing order.

Since  $y_i$  is in a discrete space, the pairwise difference is also discrete  $d_{i,i'} \in \{-1, 0, 1\}^p$ . The Laplace density function previously defined can be treated as the probability mass function at these discrete values, up to a proportional difference due to normalization. In practice, we do not find a detectable difference with or without the normalizing constant; therefore we use the algorithm of Section 3 for computation ease.

We cluster the simulated data using Bayesian distance clustering, a mixture of Bernoulli distributions as the true model, and the mixture of Gaussians as a misspecified model. Table 2 lists the clustering accuracy for  $p$  from 2 to 10. Bayesian distance clustering has good performance close to the correct Bernoulli model. The mixture of Gaussians has lower accuracy at small  $p$ . All three models have improving performance as  $p$  increases, due to the increasing separation between two clusters.

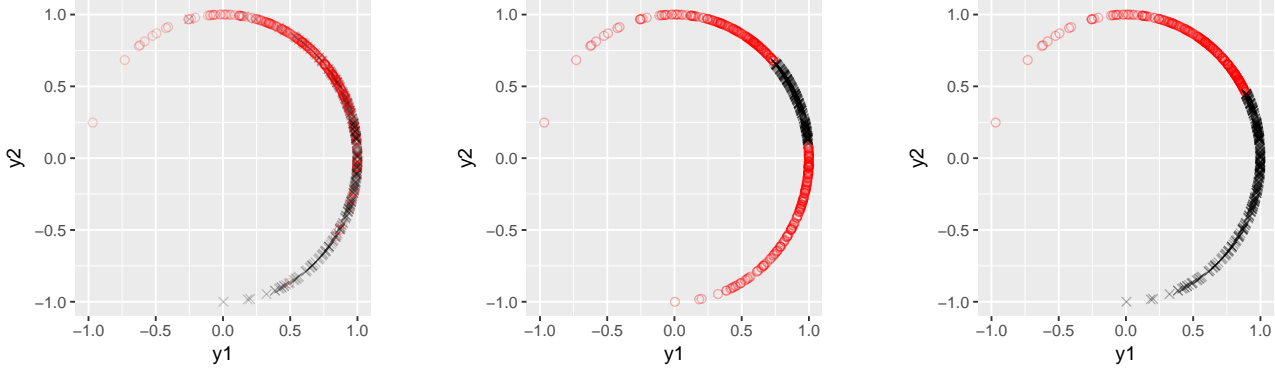
Table 2: Accuracy of clustering multivariate Bernoullis under different dimensions  $p$ . Adjusted Rand index (ARI) is computed for the point estimates using variation of information. The average ARI and 95% credible intervals are shown.

$p$	Bayes Dist. Clustering	Mix. of Gaussians	Mix. of Bernoullis
2	0.71 (0.65, 0.76)	0.66 (0.61, 0.71)	0.72 (0.65, 0.77)
3	0.72 (0.65, 0.77)	0.65 (0.62, 0.69)	0.72 (0.66, 0.77)
4	0.71 (0.64, 0.76)	0.66 (0.61, 0.72)	0.71 (0.64, 0.76)
5	0.84 (0.81, 0.87)	0.72 (0.69, 0.76)	0.84 (0.81, 0.87)
10	0.92 (0.91, 0.93)	0.92 (0.90, 0.94)	0.92 (0.92, 0.93)
20	1.00 (1.00, 1.00)	1.00 (1.00, 1.00)	1.00 (1.00, 1.00)

Next, we consider clustering data on the unit sphere  $\mathbb{S}^{p-1} = \{y : y \in \mathbb{R}^p, \|y\|_2 = 1\}$  and generate  $n = 400$  data from a two component von-Mises Fisher (vMF) mixture:

$$y_i \sim 0.5 \text{vMF}(\mu_1, \kappa_1) + 0.5 \text{vMF}(\mu_2, \kappa_2),$$

where  $y \sim \text{vMF}(\mu, \kappa)$  has density proportional to  $\exp(\kappa \mu^\top y)$ , with  $\|\mu\|_2 = 1$ . We present results for  $p = 2$ , but similar conclusions hold for  $p > 2$ . We fix  $\kappa_1 = 0.25$ ,  $\kappa_2 = 0.3$  and  $\mu_1 = (1, 0)$ , and vary  $\mu_2$  for different separation between two clusters. We measure the separation via the length of the arc between  $\mu_1$  and  $\mu_2$ . In this example, the pairwise difference is in a compact space  $d_{ii'} \in \{d : d \in [-2, 2]^2, \|d\|_2 \leq 2\}$ .



(a) Data on unit circle colored by true cluster labels. (b) Point clustering estimates from a mixture of Gaussian model. (c) Point clustering estimates from Bayesian Distance Clustering.

Figure 4: Clustering data from two-component mixture of von-Mises Fisher with  $\mu_1 = (1, 0)$  and  $\mu_2 = (1/\sqrt{2}, 1/\sqrt{2})$ . Bayesian distance clustering accurately estimates cluster labels (panel c), while mixture of Gaussians results in labels (panel b) very different from the truth.

Table 3: Accuracy of clustering spherical data. Adjusted Rand index (ARI) is computed for the point estimates using variation of information. The first parameter  $\mu_1 = (1, 0)$  is fixed and  $\mu_2$  is chosen from  $(-1, 0)$ ,  $(-\sqrt{1/5}, 2/\sqrt{5})$ ,  $(1/\sqrt{2}, 1/\sqrt{2})$  and  $(\sqrt{2/3}, 1/\sqrt{3})$ . The average ARI and 95% credible intervals are shown.

Arc-length( $\mu_1, \mu_2$ )	Bayes Dist. Clustering	Mix. of Gaussians	Mix. of vMFs
2	1.00 (1.00, 1.00)	1.00 (1.00, 1.00)	1.00 (1.00, 1.00)
1.70	0.65 (0.60, 0.70)	0.60 (0.55, 0.64)	0.65 (0.61, 0.70)
0.76	0.53 (0.43, 0.62)	0.05 (0.00, 0.10)	0.52 (0.40, 0.63)
0.61	0.40 (0.31, 0.45)	0.02 (0.00, 0.05)	0.41 (0.33, 0.45)

As shown in Table 3, as the arc-length decreases, the mixture of Gaussians starts to deteriorate rapidly. This can be explained in Figure 4(b), where the point estimate for the mixture of Gaussians treats the heavily overlapping region as one component of small variance, and outer parts as one of larger variance. Although one could avoid this behavior by constraining Gaussian components to have the same variance, this would be sub-optimal since the variances are in fact different due to  $\kappa_1 \neq \kappa_2$ . In contrast, Bayesian distance clustering accurately estimates clustering, as it encourages clustering data connected by small distances (Figure 4(c)). The result is very close to the correctly specified mixture of von Mises-Fisher distribution, as implemented in *Directional* package (Mardia and Jupp, 2009).

## 5 Clustering Brain Regions

We carry out a data application to segment the mouse brain according to the gene expression obtained from Allen Mouse Brain Atlas dataset (Lein et al., 2007). Specifically, the data are *in situ* hybridization gene expression, represented by expression volume over spatial voxels. Each voxel is a  $(200\mu m)^3$  cube. We take the mid-coronal section of  $41 \times 58$  voxels. Excluding the empty ones outside the brain, they have a sample size  $n = 1781$ . For each voxel, there are records of expression volume over 3241 different genes. To avoid the curse of dimensionality for distances, we extract the first  $p = 30$  principal components and use them as the source data.

Since gene expression is closely related to the functionality of the brain, we will use the clusters to represent the functional partitioning, and compare them in an unsupervised manner with known anatomical regions as the structural partitioning. The voxels belong to 12 macroscopic anatomical regions (Table 4).

Table 4: Names and voxel counts in 12 macroscopic anatomical structures in the coronal section of the mouse brain. They represent the *structural* partitioning of the brain.

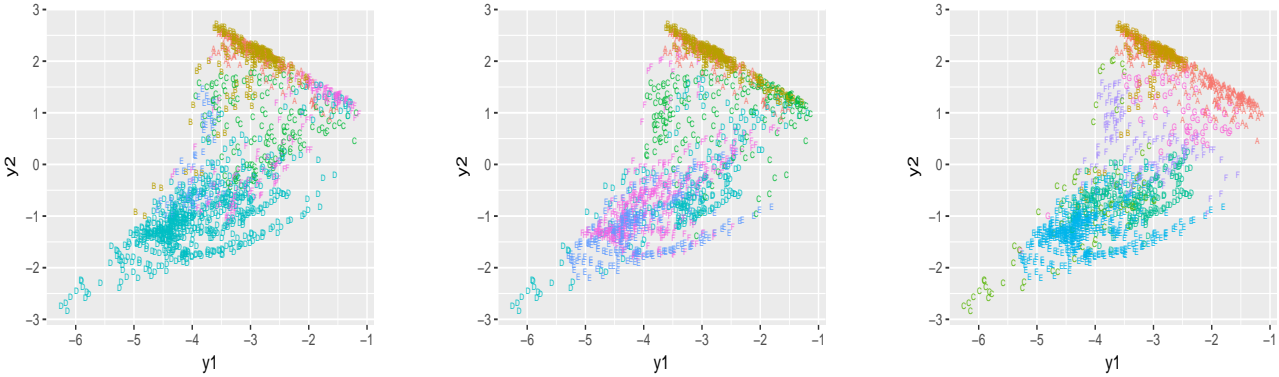
Anatomical Structure Name	Voxel Count
Cortical plate	718
Striatum	332
Thalamus	295
Midbrain	229
Basic cell groups and regions	96
Pons	56
Vermal regions	22
Pallidum	14
Cortical subplate	6
Hemispheric regions	6
Cerebellum	5
Cerebral cortex	2

For clustering, we use an overfitted mixture with  $k = 20$  and small Dirichlet concentration parameter  $\alpha = 1/20$ . As shown by Rousseau and Mengersen (2011), asymptotically, small  $\alpha < 1$  leads to automatic emptying of small clusters; we observe such behavior here in this large sample. In the Markov chain, most iterations have 7 major clusters. Table 5 lists the voxel counts at  $\hat{c}_{(n)}$ .

Table 5: Group indices and voxel counts in 7 clusters found by Bayesian Distance Clustering, using the gene expression volume over the coronal section of the mouse brain. They represent the *functional* partitioning of the brain.

Index	Voxel Count
1	626
2	373
3	176
4	113
5	79
6	39
7	12

Comparing the two tables, although we do not expect a perfect match between the structural and functional partitionings, we do see a correlation in group sizes based on the top few groups. Indeed, visualized on the spatial grid (Figure 6), the point estimates from Bayesian distance clustering have very high resemblance to the anatomical structure. Comparatively, the clustering result from Gaussian mixture model is much more different.



(a) Anatomical structure labels. (b) Point estimate from Gaussian mixture model. (c) Point estimate from Bayesian Distance Clustering.

Figure 5: Clustering mouse brain using gene expression: visualizing the clustering result on the first two principal components.



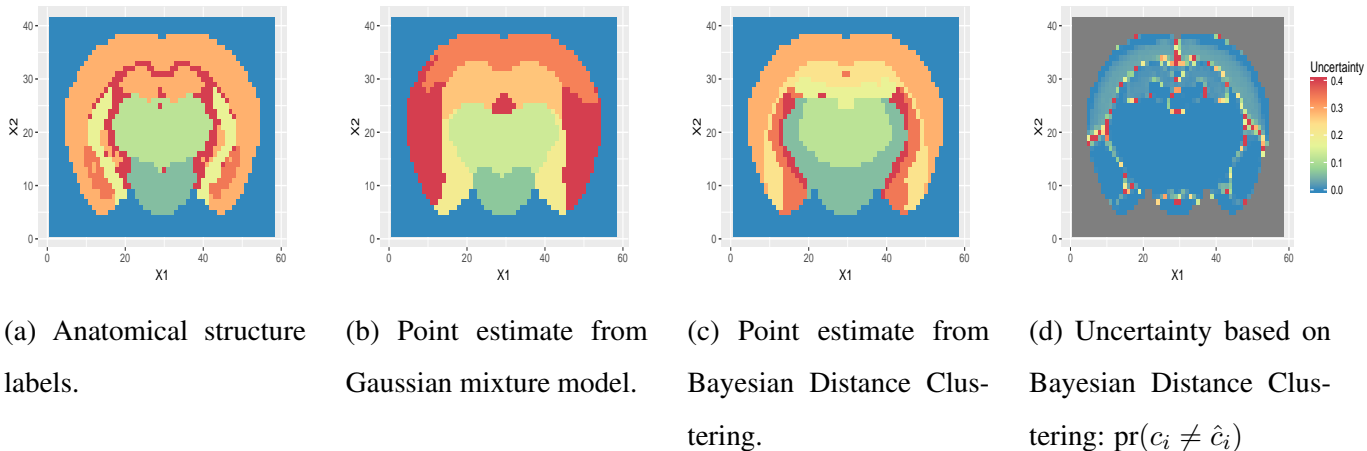


Figure 6: Clustering mouse brain using gene expression: visualizing the clustering result on the spatial grid of brain voxels. Comparing with the anatomical structure (panel a), Bayesian Distance Clustering (panel c) has higher similarity than Gaussian mixture model (panel b). Most of the uncertainty (panel d) resides in the inner layers of the cortical plate (upper parts of the brain).

Table 6: Comparison of label point estimates using Bayesian distance clustering (BDC), Gaussian mixture model (GMM), spectral clustering, DBSCAN and Mixture of Factor Analyzers. The similarity measure is computed with respect to the anatomical structure labels .

	BDC	GMM	Spectral Clustering	DBSCAN	Mix. of Factor Analyzers
Adjusted Rand Index	0.49	0.31	0.45	0.43	0.43
Normalized Mutual Information	0.51	0.42	0.46	0.44	0.47
Adjusted Mutual Information	0.51	0.42	0.47	0.45	0.47

To benchmark against other distance clustering approaches, we compute various similarity measurements and list the results in Table 6. Competing methods include spectral clustering (Ng et al., 2002), DBSCAN (Ester et al., 1996) and the mixture of factor analyzers (Ghahramani and Hinton, 1996); the first two are applied on the same dimension-reduced data as used by Bayesian distance clustering, while the last one is applied directly on the high dimensional data. Among all the methods, the point estimates of Bayesian Distance Clustering have the highest similarity to the anatomical structure.

Figure 6(d) shows the uncertainty about the point clustering estimates, in terms of the probability  $\text{pr}(c_i \neq \hat{c}_i)$ . Besides the area connecting neighboring regions, most of the uncertainty resides in the inner layers of the cortical plate (upper parts of the brain); this is due to about 30% of genes having expression concentrated only on the outer layer, leaving this part with no signals. As a result, the inner cortical plate can be either

clustered with the outer layer or with the inner striatum region.

## 6 Discussion

There are several interesting directions for future work. First, we considered each cluster to be a uni-modal distribution; hence, the pairwise distances are concentrated near zero. One could relax this assumption, by allowing the location parameter in each cluster to be a moving function, instead of a fixed point, hence the distances would concentrate near a small but non-zero constant. Second, one could consider other types of divergences, such as Kullback-Leibler or geodesic distance. This may involve optimizing the choice of metrics with additional information (Xing et al., 2003). The sensitivity to different distances is worth further study. Third, high-dimensional clustering is still a challenge. In our brain clustering application, there is a high correlation between functional and structural partitionings, allowing us to find interpretable results at the first few principal components. In general settings, this is rare since the dimension reduction usually involves loss of discriminative information (Bouveyron and Brunet-Saumard, 2014); whereas common metrics such as Euclidean distance are known to have ill behavior under large  $p$  (Beyer et al., 1999). One interesting future work is to consider fractional norm as a distance (Aggarwal et al., 2001), which has shown promising result in theory.

## Acknowledgement

This work was partially supported by grant R01-ES027498 of the United States National Institutes of Health. The authors thank Amy Herring for helpful comments on this work.

## References

- Aggarwal, C. C., A. Hinneburg, and D. A. Keim (2001). On the surprising behavior of distance metrics in high dimensional space. In *International Conference on Database Theory*, pp. 420–434. Springer.
- Banerjee, A., S. Merugu, I. S. Dhillon, and J. Ghosh (2005). Clustering with Bregman divergences. *Journal of Machine Learning Research* 6(Oct), 1705–1749.
- Beyer, K., J. Goldstein, R. Ramakrishnan, and U. Shaft (1999). When is “nearest neighbor” meaningful? In *International Conference on Database Theory*, pp. 217–235. Springer.
- Bouveyron, C. and C. Brunet-Saumard (2014). Model-based clustering of high-dimensional data: A review. *Computational Statistics and Data Analysis* 71, 52–78.

- Bregman, L. M. (1967). The relaxation method of finding the common point of convex sets and its application to the solution of problems in convex programming. *USSR Computational Mathematics and Mathematical Physics* 7(3), 200–217.
- Chernozhukov, V. and H. Hong (2003). An MCMC approach to classical estimation. *Journal of Econometrics* 115(2), 293–346.
- Coretto, P. and C. Hennig (2016). Robust improper maximum likelihood: tuning, computation, and a comparison with other methods for robust Gaussian clustering. *Journal of the American Statistical Association* 111(516), 1648–1659.
- Dunson, D. B. and J. A. Taylor (2005). Approximate Bayesian inference for quantiles. *Journal of Nonparametric Statistics* 17(3), 385–400.
- Ester, M., H.-P. Kriegel, J. Sander, and X. Xu (1996). A density-based algorithm for discovering clusters in large spatial databases with noise. In *Proceedings of the Second International Conference on Knowledge Discovery and Data Mining*, Volume 96, pp. 226–231.
- Fraley, C. and A. E. Raftery (2002, June). Model-based clustering, discriminant analysis, and density estimation. *Journal of the American Statistical Association* 97(458), 611–631.
- Ghahramani, Z. and G. E. Hinton (1996). The EM algorithm for mixtures of factor analyzers. Technical report, Technical Report CRG-TR-96-1, University of Toronto.
- Hodges, J. and E. Lehmann (1954). Matching in paired comparisons. *The Annals of Mathematical Statistics* 25(4), 787–791.
- Hoff, P. D. (2007). Extending the rank likelihood for semiparametric copula estimation. *The Annals of Applied Statistics* 1(1), 265–283.
- Jain, A. K. (2010). Data clustering: 50 years beyond K-means. *Pattern Recognition Letters* 31(8), 651–666.
- Jeffreys, H. (1961). *The Theory of Probability*. OUP Oxford.
- Johnson, V. E. (2005). Bayes factors based on test statistics. *Journal of the Royal Statistical Society: Series B (Statistical Methodology)* 67(5), 689–701.
- Juárez, M. A. and M. F. Steel (2010). Model-based clustering of non-Gaussian panel data based on skew-t distributions. *Journal of Business and Economic Statistics* 28(1), 52–66.
- Karlis, D. and A. Santourian (2009). Model-based clustering with non-elliptically contoured distributions. *Statistics and Computing* 19(1), 73–83.
- Khatri, C. and K. Mardia (1977). The von Mises-Fisher matrix distribution in orientation statistics. *Journal of the Royal Statistical Society: Series B (Statistical Methodology)* 39, 95–106.
- Lein, E. S., M. J. Hawrylycz, N. Ao, M. Ayres, A. Bensinger, A. Bernard, A. F. Boe, M. S. Boguski, K. S. Brockway, and E. J. Byrnes (2007). Genome-wide atlas of gene expression in the adult mouse brain. *Nature* 445(7124), 168.
- Li, J., S. Ray, and B. G. Lindsay (2007). A nonparametric statistical approach to clustering via mode identification. *Journal of Machine Learning Research* 8(Aug), 1687–1723.

- Mardia, K. V. and P. E. Jupp (2009). *Directional Statistics*, Volume 494. John Wiley & Sons.
- Marin, J.-M., K. Mengersen, and C. P. Robert (2005). Bayesian modelling and inference on mixtures of distributions. *Handbook of Statistics 25*, 459–507.
- Miller, J. W. and D. B. Dunson (2018). Robust Bayesian inference via coarsening. *Journal of the American Statistical Association*, in press.
- Ng, A. Y., M. I. Jordan, and Y. Weiss (2002). On spectral clustering: analysis and an algorithm. In *Advances in Neural Information Processing Systems*, pp. 849–856.
- Rand, W. M. (1971). Objective criteria for the evaluation of clustering methods. *Journal of the American Statistical Association* 66(336), 846–850.
- Rodríguez, C. E. and S. G. Walker (2014). Univariate Bayesian nonparametric mixture modeling with unimodal kernels. *Statistics and Computing* 24(1), 35–49.
- Rousseau, J. and K. Mengersen (2011). Asymptotic behaviour of the posterior distribution in overfitted mixture models. *Journal of the Royal Statistical Society: Series B (Statistical Methodology)* 73(5), 689–710.
- Stephens, M. (2000). Dealing with label switching in mixture models. *Journal of the Royal Statistical Society: Series B (Statistical Methodology)* 62(4), 795–809.
- Wade, S. and Z. Ghahramani (2018). Bayesian cluster analysis: Point estimation and credible balls. *Bayesian Analysis* 13(2), 559–626.
- Wainwright, M. J. and M. I. Jordan (2008). Graphical models, exponential families and variational inference. *Foundations and Trends in Machine Learning* 1(1–2), 1–305.
- Xing, E. P., M. I. Jordan, S. J. Russell, and A. Y. Ng (2003). Distance metric learning with application to clustering with side-information. In *Advances in Neural Information Processing Systems*, pp. 521–528.

# Appendix

## Proof of Lemma 2

*Proof.* The integral has

$$\begin{aligned}
& \int \sum_{h=1}^K \pi_h \mathcal{L}(y_{(n+1)}; c_{(n)}, c_{n+1} = h) \mathbf{d}y_{(n+1)} \\
&= \sum_{h=1}^K \pi_h \int \mathcal{L}(y_{(n+1)}; c_{(n)}, c_{n+1} = h) \mathbf{d}y_{(n+1)} \\
&= \sum_{h=1}^K \pi_h \left\{ \prod_{h' \neq h}^k G_{h'}(D_{(n_{h'}) \times (n_{h'})}^{[h']}) \right\} \\
& \quad \left\{ \int G_h(D_{(n_h+1) \times (n_h+1)}^{[h]}) \mathbf{d}d_{(n_h+1),1}^{[h]} 1(n_h > 0) + \int G_h(D_{(n_h+1) \times (n_h+1)}^{[h]}) \mathbf{d}y_1^{[h]} 1(n_h = 0) \right\} \\
&= \left( \sum_{h=1}^K \pi_h \right) \left\{ \prod_{h' \neq h}^k G_{h'}(D_{(n_{h'}) \times (n_{h'})}^{[h']}) \right\} \left\{ G_h(D_{(n_h) \times (n_h)}^{[h]}) \right\}^{1(n_h > 0)} \\
&= \mathcal{L}(y_{(n)}; c_{(n)})
\end{aligned}$$

where  $1(E)$  is the indicator function, taking 1 if condition  $E$  holds, or taking 0 otherwise; the second equation, utilizing exchangeability, assigns  $y_{n+1}$  as the  $n_h + 1$ th data point without loss of generality; the third equation uses the marginalization condition for  $n_h + 1 > 1$  and regularity condition for  $n_h + 1 = 1$ .

Multiplying  $\prod_{i=1}^n \pi_h$  on both sides and summing over  $c_{(n)}$ , the left hand side

$$\begin{aligned}
& \sum_{c_{(n)}} \prod_{i=1}^n \pi_h \int \sum_{h=1}^K \pi_h \mathcal{L}(y_{(n+1)}; c_{(n)}, c_{n+1} = h) \mathbf{d}y_{(n+1)} \\
&= \int \sum_{c_{(n+1)}} \prod_{i=1}^{n+1} \pi_h \mathcal{L}(y_{(n+1)}; c_{(n)}, c_{n+1} = h) \mathbf{d}y_{(n+1)},
\end{aligned}$$

which exchanges the summation and integral via Fubini theorem. This completes the proof.  $\square$

## Proof of Lemma 3

*Proof.* Due to the exchangeability, the marginal variance is the same for all distances

$$\text{var}(d_{i,i'}^{[h]}) \equiv \Lambda_1 \quad \forall i \neq i'$$

and the covariance is the same for all pairs of distance that shares only one datum index  $i$ :

$$\text{cov}(d_{i,i'}^{[h]}, d_{i,i''}^{[h]}) = \Lambda_2$$

where  $i, i', i''$  are three indices that are pairwise non-equal.

Using linear property of the covariance

$$\begin{aligned}
\text{cov}(d_{i,i'}^{[h]}, d_{i,i''}^{[h]}) &= \text{cov}(d_{i,i'}^{[h]}, d_{i,i'}^{[h]} - d_{i'',i'}^{[h]}) \\
&= \text{cov}(d_{i,i'}^{[h]}, d_{i,i'}^{[h]}) - \text{cov}(d_{i,i'}^{[h]}, d_{i'',i'}^{[h]})
\end{aligned}$$

yielding

$$\Lambda_2 = \Lambda_1 - \Lambda_2.$$

Therefore  $\Lambda_1 = 2\Lambda_2$ . □

## Proof of Lemma 4

*Proof.* For a clear exposition, we omit the sub/super-script  $h$  for now and use  $x_i = T(y_i)$

$$\begin{aligned} \mathbb{E}_{y_i} \mathbb{E}_{y_j} \sum_{i=1}^n \sum_{j=1}^n B_\phi(x_i, x_j) &= \mathbb{E}_{y_i} \mathbb{E}_{y_j} \sum_{i=1}^n \sum_{j=1}^n \{\phi(x_i) - \phi(x_j) - \langle x_i - x_j, \nabla \phi(x_j) \rangle\} \\ &= \mathbb{E}_{y_j} \sum_{j=1}^n \sum_{i=1}^n \{\mathbb{E}_{y_i} \phi(x_i) - \phi(\mu) - \langle \mathbb{E}_{y_i} x_i - \mu, \nabla \phi(\mu) \rangle \\ &\quad + \phi(\mu) - \phi(x_j) - \langle \mathbb{E}_{y_i} x_i - x_j, \nabla \phi(x_j) \rangle\} \\ &= n \sum_{i=1}^n \mathbb{E}_{y_i} \{\phi(x_i) - \phi(\mu) - \langle x_i - \mu, \nabla \phi(\mu) \rangle\} \\ &\quad + n \sum_{j=1}^n \mathbb{E}_{y_j} \{\phi(\mu) - \phi(x_j) - \langle \mu - x_j, \nabla \phi(x_j) \rangle\} \\ &= n \sum_{i=1}^n \mathbb{E}_y \{B_\phi(x_i, \mu) + B_\phi(\mu, x_i)\} \end{aligned}$$

where  $\langle \cdot, \cdot \rangle$  denotes dot product, the second equality is due to Fubini theorem and  $\mathbb{E}_{y_i} x_i - \mu = 0$ . □

## Proof of Lemma 5

*Proof.* For notational ease, we replace  $d_{i,i',j}^{[h]}$  by  $d_j$  in this proof.

$$\begin{aligned} \mathbb{E} \max_j d_j &= \frac{1}{t} \mathbb{E} \log \exp(t \max_j d_j) \\ &\leq \frac{1}{t} \log \mathbb{E} \exp(t \max_j d_j) \\ &= \frac{1}{t} \log \max_j \mathbb{E} \exp(td_j) \\ &\leq \frac{1}{t} \log \sum_j \mathbb{E} \exp(td_j) \\ &= \frac{1}{t} \log p \{\exp(\nu_h^2 t^2)\} \\ &= \frac{\log p}{t} + \nu_h^2 t \end{aligned}$$

for any  $|t| \in [0, 1/b_h)$ ; where the first inequality is due to Jensen's inequality, and the second is due to the max of positive numbers being less or equal to their sum.

We now minimize the function  $g(t) = \frac{\log p}{t} + \nu_h^2 t$  over  $t \in [0, \infty)$ . When  $t$  is unconstrained in  $[0, \infty)$ ,  $t^* = \sqrt{\log p}/\nu_h$  yields the minimum.

**Case 1:** when  $t^* < 1/b_h$ :

This is equivalent to  $\log p < \nu_h^2/b_h^2$ ,

$$\inf_t g(t) = g(t^*) = 2\nu_h \sqrt{\log p}$$

**Case 2:** when  $t^* \geq 1/b_h$ :

This is equivalent to  $\log p \geq \nu_h^2/b_h^2$ ,  $g(t)$  is monotonically decreasing over  $[0, 1/b_h]$ , therefore

$$\inf_t g(t) = g(1/b_h) = b_h \log p + \frac{\nu_h^2}{b_h} b_h \leq 2b_h \log p$$

where the last inequality uses  $\nu_h^2/b_h^2 \leq \log p$ .

The concentration inequality is based on each  $d_j$  is sub-exponential with bound parameter  $(\sqrt{2}\nu_h, b_h)$ , then

$$\Pr(d_j > t) \leq \exp\{-t/(2b_h)\} \quad \text{for } t > 2\nu_h^2/b_h$$

by the property of sub-exponential tail. Then it follows

$$\Pr(\max_j d_j > t) = \Pr(\bigcup_j d_j > t) \leq \sum_j \Pr(d_j > t) \leq p \exp\{-t/(2b_h)\} \quad \text{for } t > 2\nu_h^2/b_h$$

As the last step, taking  $\max_j |d_j| = \max_{j=1}^p (d_1, \dots, d_p, -d_1, \dots, -d_p)$  yields both results. □